doi.org/10.36721/PJPS/2026.40.16231.1

Study on the molecular mechanism of bone marrow mesenchymal stem cells inducing epithelial-mesenchymal transition in HPV-associated cervical cancer through activation of miR-129

Nieying Ma[1], Kaijie Xu[2] and Zhize Wang[3]*

[1]Department of Obstetrics and Gynecology, Women's Hospital, School of Medicine, Zhejiang University, Hangzhou, Zhejiang, 310006, China

[2]Department of Urology, Jinhua People's Hospital, Jinhua, Zhejiang, 321000, China

[3]Department of Urology, The First Affiliated Hospital, Zhejiang University School of Medicine, Hangzhou, Zhejiang, 310003, China

Abstract: **Background**: HPV-associated cervical cancer remains a leading cause of cancer-related death in women worldwide. The role of bone marrow mesenchymal stem cells (BMSCs) and miR-129 in tumor progression remains unclear. **Objectives**: To investigate miR-129 expression and its clinical significance in HPV-associated cervical cancer and to explore whether BMSCs regulate malignant phenotypes through miR-129. **Methods**: miR-129 expression was measured by qRT-PCR in 77 cervical cancer and 30 normal cervical tissues. Associations with clinicopathological features and overall survival (OS) were analyzed. Diagnostic value was assessed by ROC curve. Rat BMSCs were co-cultured with SiHa and HeLa cells. Following miR-129 overexpression or knockdown, cell proliferation (CCK-8, colony formation), invasion (Transwell) and expression of E-cadherin, N-cadherin and MRP1 (Western blot) were examined. **Results**: miR-129 expression was significantly higher in cervical cancer tissues than in normal controls (3.24±0.56 vs. 1.00±0.32, $P<0.05$). High miR-129 expression correlated with tumor size ≥3 cm (P=0.009), FIGO stage III-IV (P=0.0034) and lymph node metastasis (P=0.038). High expression was associated with shorter OS (median: 28.4 vs. 46.2 months; HR=2.944, 95%CI:1.484-5.842, P=0.002). The AUC was 0.788 (95%CI:0.693-0.884), with a cut-off of 1.85 (sensitivity:76.9%, specificity:70.4%). BMSC co-culture upregulated miR-129 expression (SiHa: 3.52±0.42 vs. 1.00±0.08, $P<0.01$). miR-129 overexpression promoted proliferation, colony formation and invasion, while knockdown suppressed these phenotypes. Overexpression of miR-129 reduced E-cadherin (0.42±0.05 vs. 1.00±0.08, $P<0.01$) and increased N-cadherin (2.85±0.22 vs. 1.00±0.10, $P<0.01$) and MRP1 (2.46±0.18 vs. 1.00±0.09, $P<0.01$). Knockdown of miR-129 partially reversed BMSC-induced changes in these proteins. **Conclusion**: miR-129 is significantly upregulated in HPV-associated cervical cancer and shows potential as a diagnostic and prognostic biomarker. BMSCs upregulate miR-129 in cervical cancer cells and miR-129 modulates proliferation, invasion, EMT marker expression and MRP1 expression. These findings suggest that the BMSCs/miR-129 axis may contribute to cervical cancer progression, but further *in-vivo* and mechanistic studies are needed.

Keywords: BMSCs; EMT; HPV; Infiltration; miR-129; Molecular mechanism

Submitted on 05-02-2026 – Revised on 20-05-2026 – Accepted on 21-05-2026

INTRODUCTION

Cervical cancer is the fourth most common malignancy in women worldwide and its incidence and mortality remain high in developing countries (Mune *et al*., 2026). Persistent infection with high-risk Human Papillomavirus (HPV) is the most important risk factor for cervical cancer and HPV DNA is detected in more than 95% of cervical cancer cases (Intan *et al*., 2025). Despite the widespread use of prophylactic HPV vaccines, the current treatment options for patients who have developed invasive cervical cancer still face severe challenges of recurrence and drug resistance (Maiorano *et al*., 2026; Bergman *et al*., 2025). Therefore, it is of great clinical significance to understand the molecular mechanism of cervical cancer progression and find new therapeutic targets.

Epithelial-Mesenchymal Transition (EMT) is a key biological process by which epithelial-derived malignant tumor cells acquire a mesenchymal phenotype (Popiel-Kopaczyk *et al*., 2023). During EMT, the expression of epithelial marker E-cadherin is down-regulated, while that of mesenchymal markers N-cadherin and Vimentin is up-regulated, thereby enhancing the migration, invasion, and anti-apoptotic ability of tumor cells (Li and Dou, 2022). Studies have shown (Liao *et al*., 2022; Xu *et al*., 2022) that EMT not only promotes tumor metastasis but is also closely associated with chemotherapy resistance. In cervical cancer, abnormal activation of EMT is significantly associated with poor patient prognosis, but its upstream regulatory mechanism is not fully understood (Zhang *et al*., 2023).

Tumor microenvironment plays a key role in the progression of cervical cancer. Bone Marrow

**Corresponding author:* e-mail: wangzhize@zju.edu.cn

Mesenchymal Stem Cells (BMSCs) are an important stromal component in the tumor microenvironment (Cortes-Morales *et al*., 2023). Studies have shown that BMSCs can be recruited to the tumor site and regulate the proliferation, migration, EMT and chemotherapy resistance of tumor cells by secreting cytokines, exosomes, or direct contact (Nittayaboon *et al*., 2025; Abas *et al*., 2022). However, the specific role and molecular mechanism of BMSCs in HPV-related cervical cancer are still controversial and need to be further explored.

MicroRNAs (miRNAs) are a class of non-coding RNAs of about 22 nucleotides in length that can regulate target gene expression at the post-transcriptional level (Leventakou *et al*., 2023). miR-129 is aberrantly expressed in a variety of malignant tumors and is involved in the regulation of cell proliferation, apoptosis, and EMT (Tu *et al*., 2025; Hong and He, 2025). It has been reported that miR-129 is upregulated in cervical cancer tissues (Wang *et al*., 2025), but its upstream regulatory mechanisms and its relationship with BMSCs remain unclear. Although previous studies have shown that BMSCs and miR-129 play important roles in tumor progression, no study has clarified whether BMSCs affect EMT and drug resistance in cervical cancer cells by regulating miR-129 expression. Based on this, we propose the following hypothesis: BMSCs can up-regulate miR-129 expression in cervical cancer cells, thereby inducing EMT and increasing MRP1 expression, promoting the malignant progression of cancer. To test this hypothesis, we first examined the expression of miR-129 in HPV-associated cervical cancer tissues and its clinical prognostic significance. Subsequently, the effect of BMSCs on miR-129 expression in cervical cancer cells was assessed using in *vitro* co-culture experiments. Furthermore, the roles of miR-129 in cervical cancer cell proliferation, colony formation, invasion, EMT, and MRP1 expression were investigated using miR-129 overexpression and knockdown. Finally, co-culture combined with miR-129 knockdown experiment was used to verify whether the effect of BMSCs was dependent on miR-129. The aim of this study is to clarify the mechanism of the BMSCs/miR-129 axis in HPV-related cervical cancer and to provide a theoretical basis for identifying new therapeutic targets.

MATERIALS AND METHODS

Study design and reporting

This observational study was designed and reported in accordance with the Strengthening the Reporting of Observational Studies in Epidemiology (STROBE) statement. The study protocol, including the research hypothesis, sample size estimation, inclusion/exclusion criteria, laboratory procedures, and statistical analysis plan, was established prior to data collection and is available as a supplementary file (STROBE checklist and study protocol). The STROBE checklist has been revised to accurately reflect the content of this manuscript, and all items are now reported in accordance with the actual study conduct.

Tissue and cells

This study retrospectively enrolled 77 HPV-associated cervical cancer cases and 30 normal cervical controls from the tissue bank of our hospital's laboratory. The recruitment period for tissue samples was from January 2018 to December 2020, and the data collection (including clinicopathological and follow-up data) was completed by June 2024. Seventy-seven HPV-associated cervical cancer tissue samples and 30 normal cervical tissue samples were obtained from the tissue bank of our hospital's laboratory (Table 1). Normal cervical tissues were obtained from patients who underwent hysterectomy for uterine fibroids and were pathologically confirmed to be free of tumor cells and cervical intraepithelial neoplasia (Sawaya and Smith-McCune, 2016). All cervical cancer tissues were confirmed as squamous cell carcinoma or adenocarcinoma by postoperative histopathological diagnosis (Sawaya and Smith-McCune, 2016) and were positive for high-risk HPV DNA (HPV16/18/31/33, etc.) as determined by HPV genotyping PCR (Nygard *et al*., 2014). All tissue samples were collected prior to any radiotherapy, chemotherapy, targeted therapy or immunotherapy.

Complete clinicopathological data (age, tumor size, FIGO stage (Laughlin-Tommaso *et al*., 2017), lymph node status (Hong *et al*., 2012)) and follow-up data (12-60 months, median 38.5 months) were available for the 77 cervical cancer cases. Exclusion criteria for sample selection included: concomitant other malignant tumors; severe heart, liver, kidney dysfunction or immune system disease; pregnant or lactating women; and patients who received neoadjuvant therapy before surgery. Sample size estimation was performed using PASS software (v15.0) (Bujang and Adnan, 2016). With a two-sided α=0.05, power 1-β=0.80 and expected effect size d=0.65, at least 30 samples per group were required. In this study, 77 cervical cancer tissues and 30 normal cervical tissues met the statistical requirements.

The participant selection process from the tissue bank was as follows: we first screened all available cervical tissue specimens stored in the bank between January 2018 and December 2020. Cases were then sequentially assessed against the predefined inclusion and exclusion criteria. All eligible cervical cancer cases with complete clinical and follow-up data were included consecutively during the recruitment period, without any additional random sampling or selection based on outcomes. Normal cervical tissues were selected as a convenience sample from patients who underwent hysterectomy for benign uterine fibroids during the same period, and were frequency-matched to the cancer cases by age (± 5 years) to minimize confounding.

In Press

Table 1: Related clinicopathological information of the HPV-associated cervical cancer cases.

Clinical feature	Cases	miR-129 expression		P value
		Low presentation (n=38)	High presentation(n=39)	
Age (years)				
<50	40	20	20	0.9056
>50	37	18	19	
Tumor size				
<3cm	55	32	23	0.0087^
>3cm	15	3	12	
TNM staging (FIGO)				
I-II stage	46	29	17	0.0034*
III- stage	31	9	22	
Lymph node metastasis				
Absent	52	30	22	0.035
Present	25	8	17	

Culture and selection of cells

Human cervical cancer cell lines SiHa (HPV16-positive) and HeLa (HPV18-positive) were purchased from the American Type Culture Collection (ATCC). The human normal cervical epithelial cell line HcerEpic was purchased from Guangzhou Saiku Biotechnology Co., Ltd. All cells were cultured in DMEM high-glucose medium (HyClone) containing 10% fetal bovine serum (Gibco), 100 U/mL penicillin, and 100 μg/mL streptomycin in an incubator with 5% CO_2 at 37 °C and a saturated humidity. Cells were subcultured every 2-3 days and cells in the logarithmic growth phase were used for experiments. The third to eighth passage (P3-P8) cells were used in all experiments.

Detection on surface marker of BMSCs

Bone marrow from the tibia and femur of 4-week-old male Sprague-Dawley rats (SPF grade, weighing 80-100g) purchased from the Laboratory Animal Center of Zhejiang University. BMSCs were isolated by whole bone marrow adherent method: the metaphysis was cut under sterile conditions, the bone marrow cavity was repeatedly washed with L-DMEM medium (containing 10% fetal bovine serum and 1% double antibody) and the cell suspension was collected and seeded in T25 culture flask. Non-adherent cells were removed by the first exchange after 48 hours and the fluid was changed every 3 days thereafter. When the confluence of cells reached 80%-90%, the cells were digested with 0.25% trypsin (containing 0.02% EDTA) and passaged, and this was recorded as the P1 generation. P3-P5 generation cells were used for all functional experiments. P3 generation BMSCs were collected for flow cytometry to identify surface markers: After washing twice with PBS, the cell density was adjusted to 1×10^6 cells /mL and FITC-CD90 (1:100), PE-CD73 (1:100) and APC-CD105 (1:100) were added as positive markers, respectively. FITC-CD34 (1:100) and PE-CD45 (1:100) were used as negative markers, and the corresponding isotype control (FITC/PE/APC-labeled mouse IgG) was used as a negative control. After incubation at 4°C in the dark for 30 min and washing twice with PBS, the cells were analyzed by flow cytometry (BD FACSCalibur), and the positive rate was analyzed using FlowJo v10 software. The identification criteria for BMSCs were as follows (Gao *et al* ., 2022): the positive rates of CD90, CD73, and CD105 were more than 95%, and the positive rates of CD34 and CD45 were less than 2%.

Cell transfection

miR-129 mimic, miR-129 inhibitor, and their corresponding negative controls (NC mimic, NC inhibitor) were purchased from Guangzhou Ribobio Co., Ltd. Sequence information is as follows: The sense chain of miR-129 mimic was 5'-CUUUUUGCGGUCUG GGCUUGC-3' and the sequence of miR-129 inhibitor was 5'-GCAAGCCCAGACCGCCAAAAAG-3'. The sense chain of NC mimic was 5'-UUCUCCGAACGUGUC ACGUTT-3'. Follow the instructions for Lipofectamine 3000 (Invitrogen, L3000015): SiHa or HeLa cells were seeded in 6-well plates (2×10^5 cells/well), and when the confluence reached 70% to 80%, liposomes and nucleic acids were diluted in Opti-MEM medium (Gibco) to a final concentration of 50 nM. Six hours after transfection, the culture was replaced with complete medium and incubated for an additional 48 hours. Two methods verified transfection efficiency: qRT-PCR to detect miR-129 expression levels, and independent transfection experiments using a FAM-labeled NC mimic, with the proportion of green fluorescence-positive cells observed under a fluorescence microscope 24 hours after transfection indicating a transfection efficiency of about 75% to 85%. Only batches with transfection efficiency >70% were selected for subsequent functional experiments.

Presentation level of miR-129 detected with qRT-PCR (Jeong et al., 2022)

Total RNA was extracted from tissues or cells using TRIzol reagent (Invitrogen). RNA concentration and purity (A260/A280 ratio between 1.8 and 2.0) were determined

Article in Press

by NanoDrop 2000. RNA was reverse transcribed into cDNA using the miRNA reverse transcription kit (TaKaRa, product number 638313). qPCR reactions were performed using SYBR Green Master Mix (TaKaRa, item number RR820A) on an ABI 7500 system. U6 was used as the reference gene. The primer sequence was as follows: F of miR-129-5p was 5'-CGCGCGCTTTTTGCGGTCTGG-3', R was 5'-GTGCAGGGTCCGAGGT-3'. U6 F is 5'-CTCGCTTCGGCAGCACA-3' and R is 5'-AACGCTTCACGAATTTGCGT-3'. Reaction conditions: predenaturation at 95°C for 5 minutes; There were 40 cycles of denaturation at 95°C for 15 seconds followed by annealing/extension at 60°C for 60 seconds. Three complex Wells were set for each sample. The relative expression of miR-129 was calculated using the $2^{-}\Delta\Delta Ct$ method and normalized using U6 as an internal reference.

Co-culture system of BMSCs and cervical cancer cells

The Transwell non-contact co-culture system (Corning, pore size 0.4 μm, catalog number 3412) was adopted. This pore size allows soluble factors, such as cytokines and exosomes, to pass freely, but prevents direct contact between the two cell types. The specific procedure was as follows: BMSCs (P3-P5 generation) were seeded at 1×10^5 cells/well in the lower chamber (24-well plate) and cultured for 24 hours to make them adhere to the wall. The transfected SiHa or HeLa cells were seeded into the upper chamber (Transwell chamber) at 2×10^5 cells/well. The same DMEM complete medium (10% FBS) was used in the upper and lower chambers. After 48 hours of co-culture, cervical cancer cells in the upper chamber were collected for subsequent functional experiments. In the control group, cervical cancer cells were cultured alone (without adding BMSCs; the upper chamber was cultured in another 24-well plate, and the medium and culture conditions were the same). The timing of transfection and co-culture in this experiment was as follows: miRNA transfection (48 hours after transfection) was performed first and BMSCs co-culture (48 hours after co-culture) was performed, that is, cells were inoculated on Day 0, transfected on Day 1, co-culture was started after verifying transfection efficiency on Day 3 and cells were collected on Day 5 for functional detection. To explore whether BMSCs regulated the malignant phenotype of cervical cancer cells depends on miR-129, the following groups were set up: Control group (cervical cancer cells cultured alone, No BMSCs), BMSCs group (cervical cancer cells +BMSCs co-culture), BMSCs+miR-NC group (cervical cancer cells transfected with NC inhibitor +BMSCs co-culture), BMSCs+miR-129 inhibitor group (cervical cancer cells transfected with miR-129 inhibitor +BMSCs co-culture).

Cell proliferation assay (CCK-8)

The treated SiHa or HeLa cells were seeded in 96-well plates at 5×10^3 cells/well and each group had 6 multiple Wells. After 24, 48, 72 and 96 hours of culture, 10 μL CCK-8 reagent (Dojindo, CK04) was added to each well and incubated for 1.5 hours at 37 ° C. The absorbance (OD) at 450 nm was measured using a microplate reader (Bio-Rad iMark). The experiments were repeated three times independently.

Colony formation experiment

The processed cells were inoculated at 500 cells per well into 6-well plates, with 3 replicate wells in each group. The cultures were incubated for 14 days (with the medium changed every 3 days) until visible colonies could be observed. The cells were washed twice with PBS, fixed with 4% paraformaldehyde for 15 minutes and stained with 0.1% crystal violet for 20 minutes. The colonies containing ≥ 50 cells were counted under an inverted microscope. The experiment was independently repeated 3 times.

Transwell invasion assay

First, the Matrigel matrix gel (BD Biosciences, item number 356234) was diluted 1:8 with serum-free DMEM. Then, 50 μL was coated onto the upper chamber of a Transwell (8 μm pore size, Corning, item number 3422) and allowed to solidify at 37°C for 30 minutes. In the upper chamber, a cell suspension without FBS (1×10^5 cells/200 μL) was added, while the lower chamber was filled with DMEM medium containing 20% FBS as the chemoattractant. After 24 hours of culture, the cells that did not migrate in the upper chamber were wiped off with a cotton swab. The cells in the lower chamber were fixed with 4% paraformaldehyde for 15 minutes and stained with 0.1% crystal violet for 20 minutes. Under an inverted microscope, 5 random fields (×200) were selected for counting the number of migrated cells. The experiment was independently repeated 3 times.

Western blot experiment (Mishra, 2022)

The total protein of the cells was extracted using RIPA lysis buffer (containing protease and phosphatase inhibitors, Beyotime, catalog number P0013K). The protein concentration was determined by BCA method (Beyotime, catalog number P0012) and a standard curve was plotted. 30 μg of protein was subjected to 10% SDS-PAGE electrophoresis (80V for 30 minutes; 120V for 60 minutes) and then transferred to a PVDF membrane (Millipore, catalog number IPVH00010) using the wet transfer method (300 mA for 90 minutes). The membrane was incubated at room temperature with 5% skimmed milk (TBST prepared) for 1 hour. The primary antibodies (diluted in 5% BSA-TBST) were added and incubated at 4°C overnight. The information of the primary antibodies is as follows: Rabbit anti-human E-cadherin (1:1000, Cell Signaling, catalog number 3195S), rabbit anti-human N-cadherin (1:1000, Abcam, catalog number ab18203), rabbit anti-human MRP1/ABCC1 (1:500, Santa Cruz, catalog number sc-13135), mouse anti-human GAPDH (1:5000, Abcam, catalog number ab8245). The membrane was washed with TBST 5 times for 5 minutes each. The secondary antibody

Article in Press

labeled with HRP (1:5000, Jackson ImmunoResearch) was added and incubated at room temperature for 1 hour. The membrane was washed with TBST 5 times for 5 minutes each. The chemiluminescence method ECL was used for imaging (Bio-Rad ChemiDoc XRS+ system). The gray-scale analysis of the bands was performed using ImageJ software (v1.53) to represent the relative expression level as the gray-scale ratio of the target protein to the internal reference GAPDH. The experiment was independently repeated 3 times.

Bioinformatics prediction

The potential target genes of miR-129-5p were predicted using the TargetScan (v8.0), miRDB (v6.0) and miRTarBase (v9.0) databases. The selection criteria were: simultaneously predicted in at least two databases, with binding sites conserved across mammals, and target genes protein-coding. The predicted target genes were then imported into the DAVID database (v6.8) for GO functional annotation and KEGG pathway enrichment analysis ($P < 0.05$ was considered significant enrichment), with a focus on pathways related to EMT, cell proliferation and drug resistance.

Experimental repetition and quality control

All *in-vitro* cell experiments were independently repeated three times, with different batches of cells and reagents used in each experiment. For qRT-PCR, each sample was run in triplicate; for Western blot, two replicates were used per sample. The figure shows the results of one representative experiment. The data in the column and line charts are the mean ± standard deviation from three independent experiments. During colony counting, Western blot gray-scale analysis and Transwell migration cell counting, blind counting was performed by researchers unfamiliar with the experimental groups to reduce bias.

Statistical analysis

Statistical analysis was performed using SPSS 26.0 and GraphPad Prism 9.0 software. All data were presented as mean ± standard deviation (Mean ± SD). Before conducting parametric tests on all continuous variables, the Shapiro-Wilk normality test and the Levene homogeneity-of-variance test were performed. Data that followed a normal distribution and had homogeneous variances were analyzed using two-tailed t-tests; one-way analysis of variance was used and pairwise comparisons were conducted using Tukey's HSD test or Games-Howell test. All tests involving multiple pairwise comparisons were adjusted for significance using the Bonferroni method. Survival curves were plotted using the Kaplan-Meier method and comparisons between groups were performed using the Log-rank test; single-factor Cox regression was used to evaluate the impact of each variable on overall survival; variables with $P < 0.10$ in the single-factor analysis were included in the multivariate Cox regression model and the forward stepwise regression method was used to calculate the hazard ratio (HR) and 95% confidence interval (CI). In the multivariate Cox regression model, confounders were selected based on clinical relevance (age, tumor size, FIGO stage, and lymph node metastasis) and statistical significance in univariate analysis ($P<0.10$). The final model included tumor size, FIGO stage, lymph node metastasis, and miR-129 expression as covariates. Age was not included in the final model because it was not significant in univariate analysis ($P=0.58$) and its inclusion did not change the effect estimates for miR-129 by more than 10%, indicating minimal confounding. The receiver operating characteristic (ROC) curve was used to evaluate the diagnostic efficacy of miR-129 expression for cervical cancer and the area under the curve (AUC), 95% confidence interval (CI), Youden index, optimal cut-off value, sensitivity and specificity were calculated. All tests were two-tailed and $P < 0.05$ was considered statistically significant.

RESULTS

Identification on BMSCs

The rat BMSCs were successfully isolated and cultured using the whole bone marrow adherent method. Under an inverted microscope, the primary BMSCs began to adhere 24 hours after inoculation, presenting a long spindle-shaped or polygonal morphology; on the 3rd day of culture, the cell fusion rate reached 50%-60%; and on the 7th-10th days, it could reach 80%-90% fusion (Fig. 1A). The results of flow cytometry identification showed that the P3 generation BMSCs highly expressed the positive markers of mesenchymal stem cells CD90 (97.20%), CD73 (96.50%) and CD105 (95.80%), while expressing low levels of hematopoietic cell markers CD34 (2.10%) and CD45 (1.80%) (Fig. 1B). These results are in line with the typical immunophenotypic characteristics of BMSCs (positive markers >95%, negative markers <2%), indicating that high-purity BMSCs were successfully obtained for subsequent co-culture experiments.

The expression and clinical significance of miR-129 in HPV-related cervical cancer tissues

The qRT-PCR results showed that the expression level of miR-129 in 77 HPV-related cervical cancer tissues was significantly higher than that in 30 normal cervical tissues ($P < 0.05$, Fig. 2A). Based on the median expression level of miR-129 (1.85), the 77 cases were divided into a high-expression group ($n = 39$) and a low-expression group ($n = 38$). The clinical-pathological feature analysis (Table 1) showed that high expression of miR-129 was significantly associated with larger tumor size ($\geqslant$ 3 cm, $P = 0.009$), advanced FIGO stage (III-IV, $P = 0.0034$), and lymph node metastasis ($P = 0.038$).

Article in Press

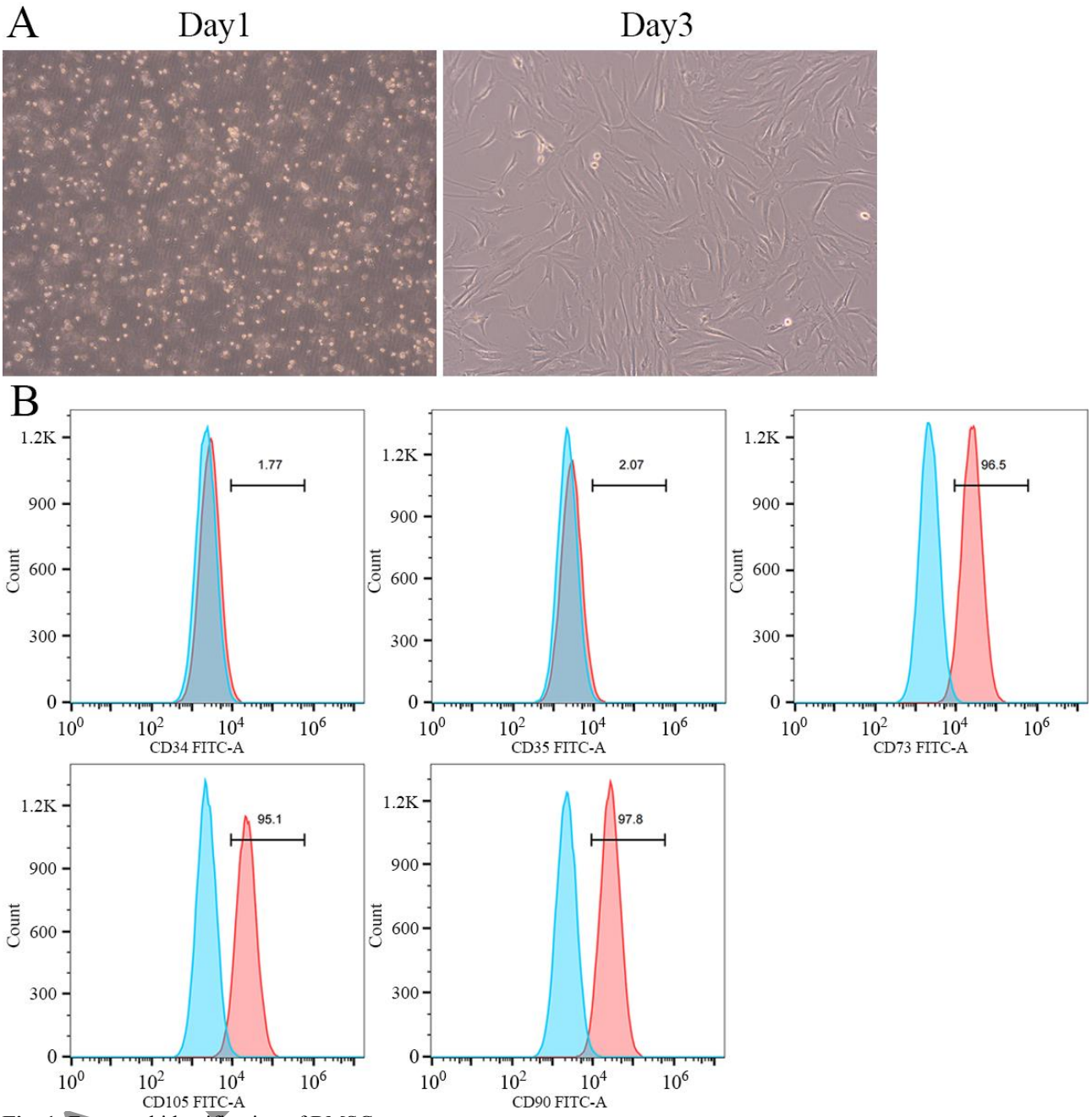


Fig. 1: Form and identification of BMSCs
A: there was long shuttle in primary BMSCs at the first day and third day of cell growth (magnification times: 200); B: surface antigen of BMSCs identified with FCM including negative antigen as CD34 (2.10%),CD45(1.80%) and positive antigen as CD90 (97.20%), CD73 (96.50%), CD105 (95.80%).

Table 2: Results of univariate and multivariate Cox regression analysis.

Variable	Univariate analysis		Multivariate analysis	
	HR (95% CI)	P	Adjusted HR (95% CI)	P
High expression of miR-129 (vs. low expression)	2.944(1.484-5.842)	0.002	2.512(1.232-5.124)	0.011
Tumor size ≥ 3 cm (vs. < 3 cm)	2.521(1.287-4.938)	0.007	2.103(1.025-4.312)	0.042
FIGO stage III-IV (vs. I-II stage)	3.124(1.623-6.014)	0.001	2.876(1.412-5.856)	>0.05
Positive lymph node metastasis (vs. negative)	2.876(1.398-5.914)	0.004	2.345(1.087-5.062)	0.030

Indicators	Numerical value	95% CI
Area under the curve (AUC)	0.7881	0.6925-0.8837
Optimal cut-off value	1.85	-

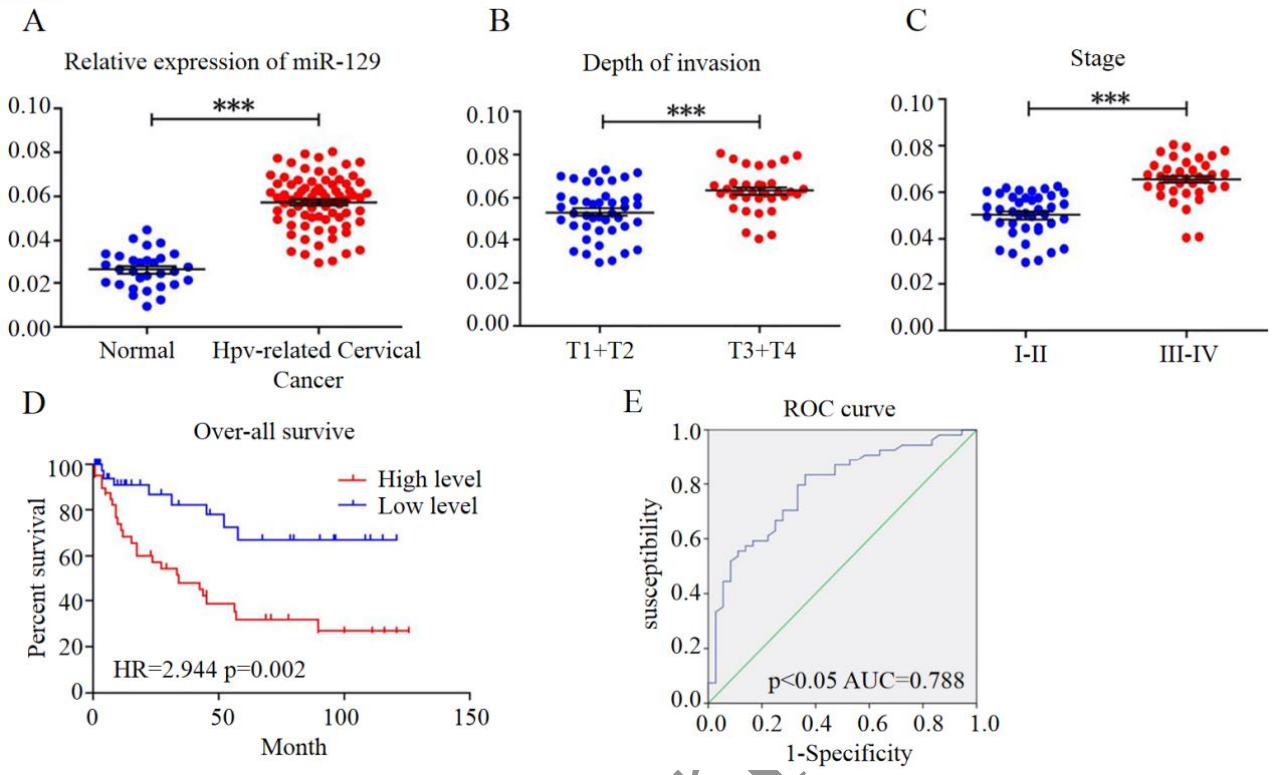


Fig. 2: High expression of miR-129 in HPV-associated cervical cancer
A: expression level of miR-129 in cervical cancer tissue was higher than in normal control group notably (***: P < 0.001); B: expression level of miR-129 in cervical cancer tissue of cases at infiltrated T3 and T4 stage was higher than in T1 and T2 stage (***: P < 0.01); C: expression level of miR-129 in cervical cancer tissue of cases at FIGO stage III and IV was higher than at stage I and II (***: P < 0.01); D: overall survival time in group with high expression of miR-129 was shorter than in group with low expression notably (HR = 2.944, 95% CI: 1.484-5.842, Log-rank P = 0.002); E: ROC curve between expression quantity of miR-129 and diagnostic sensitivity of cervical cancer (AUC = 0.788, 95% CI: 0.693-0.884, P < 0.001).

Table 3: Diagnostic value of miR-129 expression for HPV-associated cervical cancer (ROC curve analysis).

Indicator	Value	95% CI
AUC	0.788	0.693–0.884
P value	< 0.001	—
Optimal cut-off value	1.85	—
Youden index	0.473	—
Sensitivity	76.9%	60.70%–88.90%
Specificity	70.4%	49.80%–86.20%

The survival analysis indicated that the median overall survival (OS) was significantly shorter in the high-miR-129 group (28.4 months vs. 46.2 months). The Kaplan-Meier survival curve showed that the cumulative survival rate of the high-expression group was significantly lower than that of the low-expression group (Log-rank P = 0.002, Fig. 2D). Univariate Cox regression analysis showed that high expression of miR-129 (HR = 2.944, 95% CI: 1.484-5.842, P = 0.002), tumor size ≥ 3 cm (HR = 2.521, 95% CI: 1.287-4.938, P = 0.007), FIGO stage III-IV (HR = 3.124, 95% CI: 1.623-6.014, P = 0.001) and positive lymph node metastasis (HR = 2.876, 95% CI: 1.398-5.914, P = 0.004) were all risk factors for OS. Further inclusion of the above variables in the multivariate Cox regression model showed that high expression of miR-129 was an independent prognostic risk factor for OS (adjusted HR = 2.512, 95% CI: 1.232-5.124, P = 0.011) (Table 2).

The ROC curve analysis results showed that the area under the curve (AUC) for differentiating HPV-related cervical cancer cases from normal controls based on miR-129 expression level was 0.788 (95% CI: 0.693-0.884, P < 0.001) (Fig. 2E). The optimal cut-off value determined by the maximum Youden index (0.473) was 1.85, corresponding to a sensitivity of 76.9% (95% CI: 60.70%-88.90%) and a specificity of 70.4% (95% CI: 49.80%-86.20%) (Table 3).

Article in Press

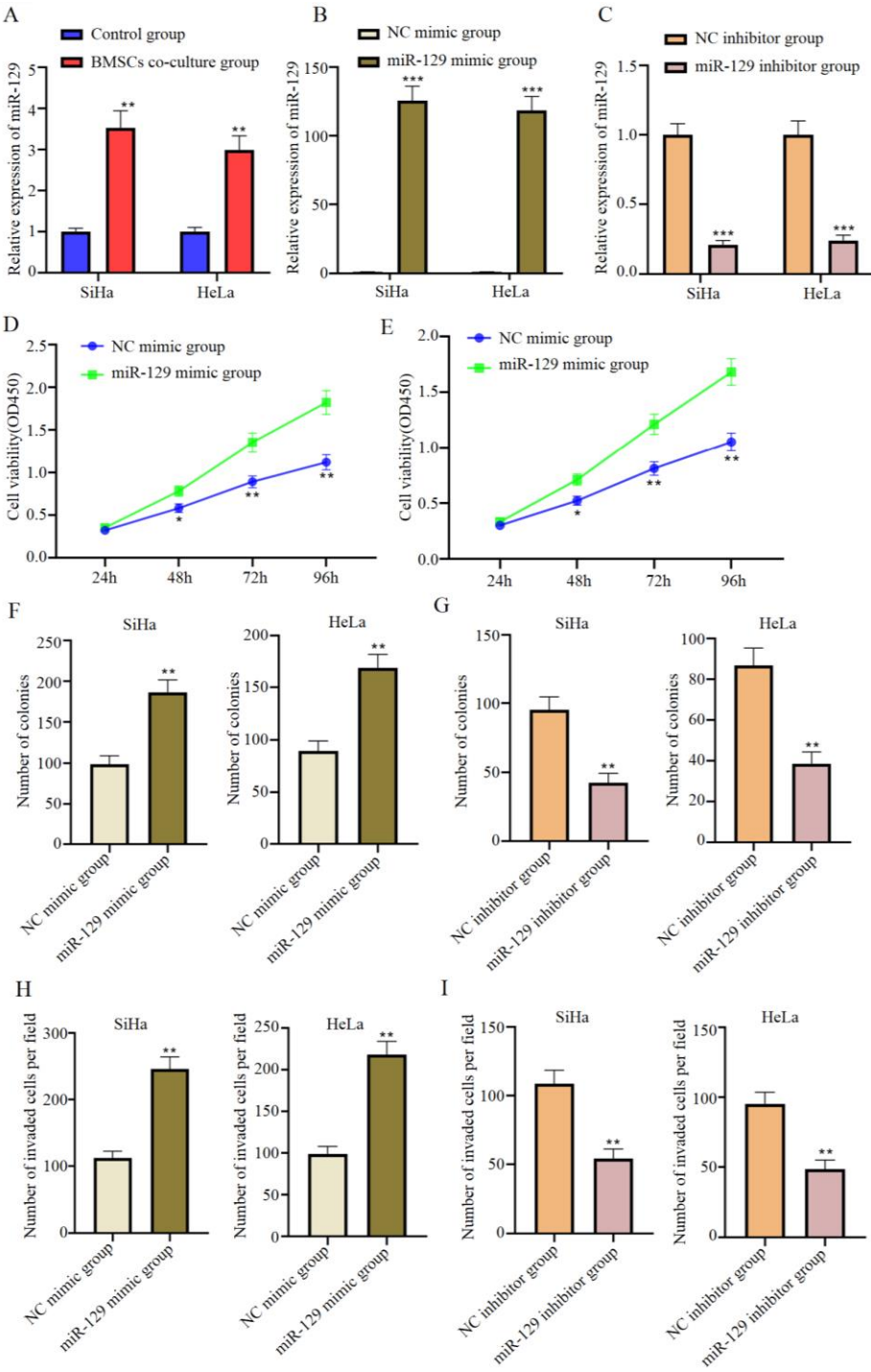


Fig. 3: BMSCs promote the proliferation, colony formation and invasion of cervical cancer cells by upregulating miR-129 expression

A: expression level of miR-129 in SiHa and HeLa cell lines co-cultured with BMSCs (**: $P < 0.01$); B: transfection efficiency of miR-129 mimic in SiHa and HeLa cells (***: $P < 0.001$); C: transfection efficiency of miR-129 inhibitor in SiHa and HeLa cells (***: $P < 0.001$); D: cell proliferation activity detected by CCK-8 after overexpression of miR-129 in SiHa cells (*: $P < 0.05$, **: $P < 0.01$); E: cell proliferation activity detected by CCK-8 after overexpression of miR-129 in HeLa cells (*: $P < 0.05$, **: $P < 0.01$); F: colony formation ability after overexpression of miR-129 in SiHa and HeLa cells (**: $P < 0.01$); G: colony formation ability after knockdown of miR-129 in SiHa and HeLa cells (**: $P < 0.01$); H: invasion ability after overexpression of miR-129 in SiHa and HeLa cells (**: $P < 0.01$); I: invasion ability after knockdown of miR-129 in SiHa and HeLa cells (**: $P < 0.01$).

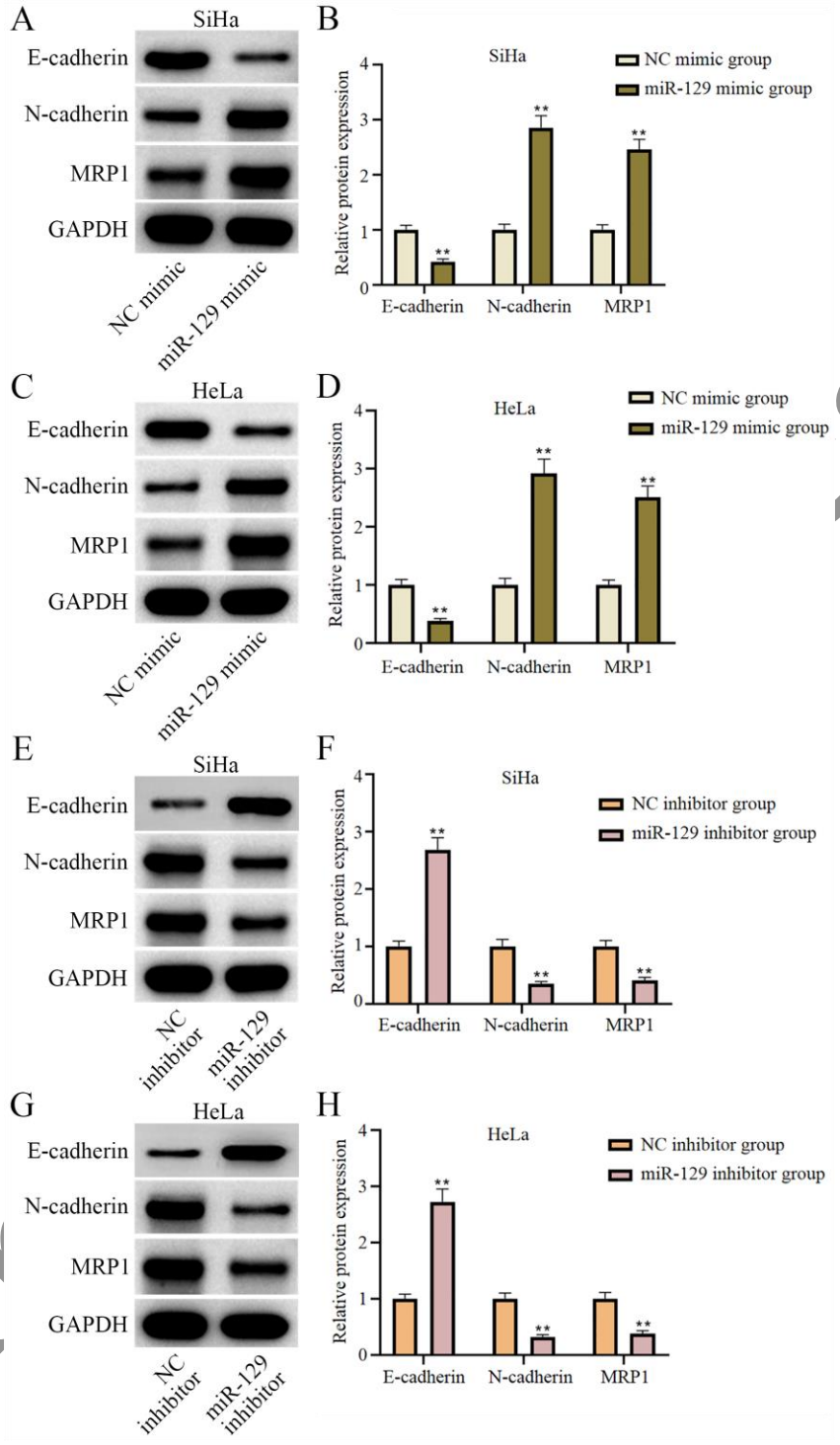


Fig. 4: Correlation between miR-129 expression and EMT markers as well as the drug resistance-related protein MRP1. A: Western blot bands of E-cadherin, N-cadherin, MRP1 and GAPDH in SiHa cells after overexpression of miR-129; B: gray scale quantification of Western blot results in SiHa cells after overexpression of miR-129 (**: $P < 0.01$); C: Western blot bands of E-cadherin, N-cadherin, MRP1 and GAPDH in HeLa cells after overexpression of miR-129; D: gray scale quantification of Western blot results in HeLa cells after overexpression of miR-129 (**: $P < 0.01$); E: Western blot bands of E-cadherin, N-cadherin, MRP1 and GAPDH in SiHa cells after knockdown of miR-129; F: gray scale quantification of Western blot results in SiHa cells after knockdown of miR-129 (**: $P < 0.01$); G: Western blot bands of E-cadherin, N-cadherin, MRP1 and GAPDH in HeLa cells after knockdown of miR-129; H: gray scale quantification of Western blot results in HeLa cells after knockdown of miR-129 (**: $P < 0.01$).

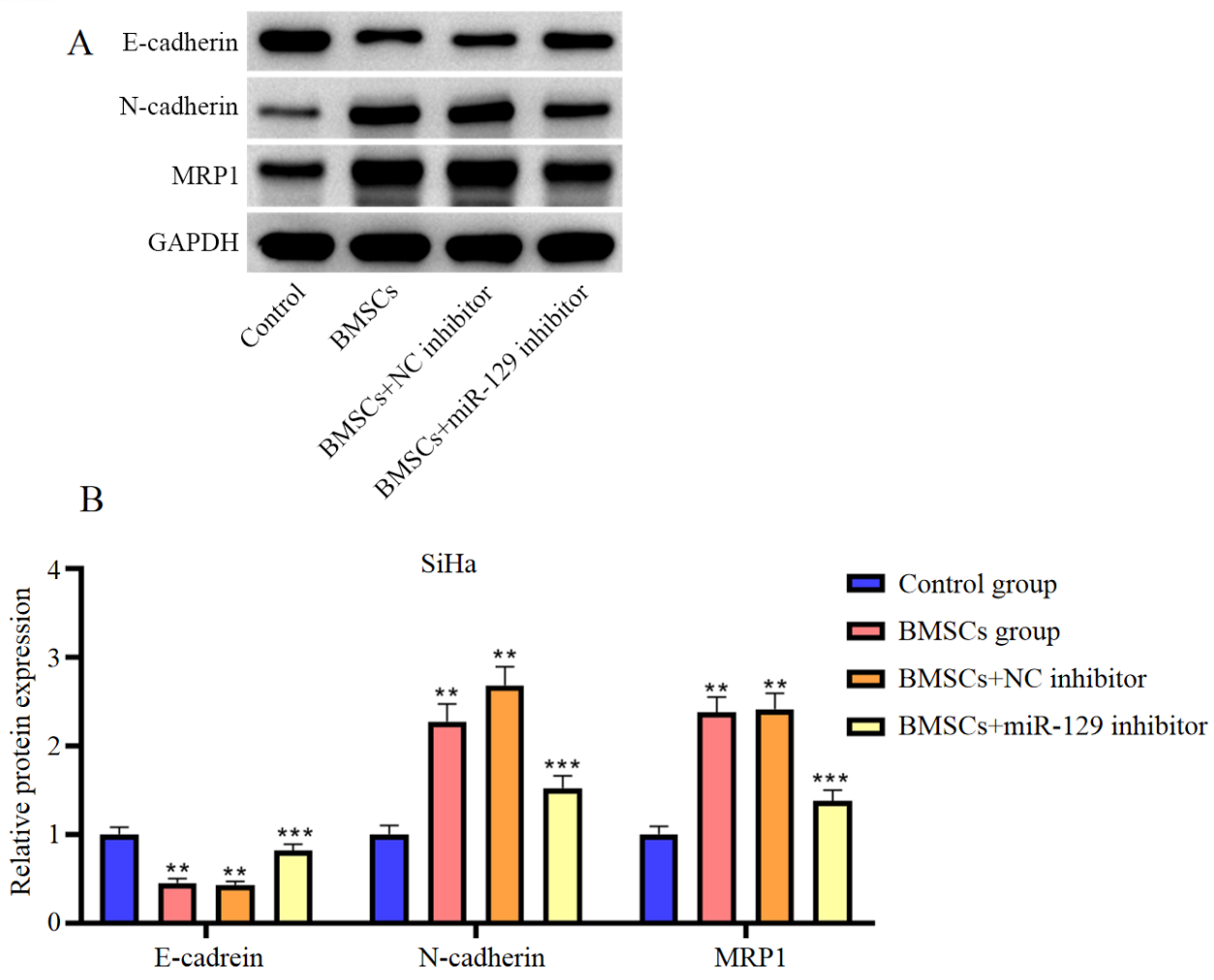


Fig. 5: The effect of BMSCs on EMT markers and MRP1 expression in cervical cancer cells is partially dependent on miR-129.
A: Western blot bands of E-cadherin, N-cadherin, MRP1 and GAPDH in SiHa cells of control group, BMSCs group, BMSCs+NC inhibitor group and BMSCs+miR-129 inhibitor group; B: gray scale quantification of Western blot results in SiHa cells of four groups (**: $P < 0.01$ vs. control group;***: $P < 0.05$ vs. BMSCs+NC inhibitor group).

BMSCs promote the proliferation of HPV-related cervical cancer cells by activating the high expression of miR-129.

The results of qRT-PCR showed that compared with the control group (cultured alone), co-culture with BMSCs significantly upregulated the expression level of miR-129 in SiHa cells ($P < 0.01$) and HeLa cells ($P < 0.01$) (Fig. 3A). This indicates that BMSCs can promote the expression of miR-129 in cervical cancer cells.

The influence of miR-129 expression level on the proliferation, colony formation and invasion ability of cervical cancer cells

To investigate the function of miR-129 in cervical cancer cells, miR-129 mimic, miR-129 inhibitor and their corresponding negative controls were transfected into SiHa and HeLa cells respectively. The results of qRT-PCR verification showed that the expression level of miR-129 in the miR-129 mimic transfection group was significantly higher than that in the NC mimic group ($P < 0.001$, Fig. 3B), while the expression level of miR-129 in the miR-129 inhibitor transfection group was significantly lower than that in the NC inhibitor group ($P < 0.001$, Fig. 3C), indicating good transfection efficiency.

The CCK-8 experiment results showed that after overexpression of miR-129, the proliferation activity of SiHa and HeLa cells at 48 hours, 72 hours and 96 hours was significantly higher than that of the NC mimic group ($P < 0.05$ or $P < 0.01$, Fig. 3D); conversely, after knockdown of miR-129, the proliferation activity of the cells at each time point was significantly lower than that of the NC inhibitor group ($P < 0.05$ or $P < 0.01$, Fig. 3E).

Article

The colony formation experiment results showed that the number of colonies formed in the miR-129 overexpression group was significantly higher than that in the NC mimic group (SiHa: 186.3 ± 15.2 vs. 98.7 ± 10.4, P < 0.01; HeLa: 168.5 ± 12.8 vs. 89.3 ± 9.6, P < 0.01, Fig. 3F); while the number of colonies formed in the miR-129 knockdown group was significantly lower than that in the NC inhibitor group (SiHa: 42.6 ± 6.8 vs. 95.2 ± 9.3, P < 0.01; HeLa: 38.4 ± 5.9 vs. 86.7 ± 8.5, P < 0.01, Fig. 3G).

The Transwell invasion experiment results showed that the number of cells passing through the basement membrane in the miR-129 overexpression group was significantly higher than that in the NC mimic group (SiHa: 245.6 ± 18.3 vs. 112.4 ± 10.2, P < 0.01; HeLa: 218.3 ± 15.6 vs. 98.5 ± 9.4, P < 0.01, Fig. 3H); while the number of cells passing through the basement membrane in the miR-129 knockdown group was significantly lower than that in the NC inhibitor group (SiHa: 54.2 ± 7.1 vs. 108.6 ± 9.8, P < 0.01; HeLa: 48.7 ± 6.5 vs. 95.3 ± 8.2, P < 0.01, Fig. 3I).

The correlation between the expression level of miR-129 and the expression of EMT markers as well as the drug resistance-related protein MRP1

In SiHa cells, compared with the NC mimic group, the expression level of the epithelial marker E-cadherin in the miR-129 overexpression group was significantly decreased (P < 0.01), while the expression level of the mesenchymal marker N-cadherin was significantly increased (P < 0.01) and the expression level of the drug resistance-related protein MRP1 was also significantly increased (P < 0.01) (Figs. 4A-B). In HeLa cells, similar results were obtained upon miR-129 overexpression (Figs. 4C-D).

Conversely, in SiHa cells, compared with the NC inhibitor group, the expression level of E-cadherin in the miR-129 knockdown group was significantly increased (P < 0.01), while the expression levels of N-cadherin and MRP1 were both significantly decreased (P < 0.01) (Figs. 4E-F). In HeLa cells, similar results were obtained following miR-129 knockdown (Figs. 4G-H).

The influence of BMSCs on the EMT markers and MRP1 expression of cervical cancer cells is partially dependent on miR-129.

To further verify whether the effect of BMSCs on cervical cancer cells depends on miR-129, SiHa cells transfected with miR-129 inhibitor or NC inhibitor were co-cultured with BMSCs for 48 hours. The results of Western blot (Figs. 5A-B) showed that compared with the control group, the expression of E-cadherin was decreased and the expressions of N-cadherin and MRP1 were increased in the BMSCs co-culture group. Compared with the BMSCs + NC inhibitor group, the expression level of E-cadherin in the BMSCs + miR-129 inhibitor group was partially increased, while the expression levels of N-cadherin and MRP1 were partially decreased.

Bioinformatics predicts the potential target genes and signaling pathways of miR-129

To explore the possible downstream molecular mechanism of miR-129, the potential target genes of miR-129-5p were predicted using the TargetScan, miRDB and miRTarBase databases. The intersection results of the three databases showed that the candidate target genes included SPARC, ZIC2, PAX3, SOCS4, etc., totaling 28 genes (Fig. 6A). The KEGG pathway enrichment analysis revealed that these target genes were significantly enriched in the PI3K/Akt signaling pathway, Wnt signaling pathway, NF-κB signaling pathway, MAPK signaling pathway, adhesion connection pathway and ECM-receptor interaction (P < 0.05, Fig. 6B).

DISCUSSION

Cervical cancer is one of the most common malignant tumors in the female reproductive system. Persistent HPV infection is a necessary factor for its occurrence. Although the widespread use of HPV screening and vaccines has significantly reduced the incidence of cervical cancer, HPV-related cervical cancer still accounts for over 90% of global cervical cancer cases (Kusakabe *et al*., 2023) and recurrence, metastasis and chemotherapy resistance remain the main causes of treatment failure and patient death. The tumor microenvironment plays a crucial role in the progression of cervical cancer and BMSCs, as an important component of the microenvironment, can regulate the malignant phenotype of tumor cells by secreting exosomes, cytokines, etc. (Wang *et al*., 2024). However, whether and how BMSCs promote the progression of HPV-related cervical cancer by regulating miRNA expression is currently unclear. This study aims to investigate the effects of BMSCs on the proliferation, invasion, EMT and drug resistance of HPV-related cervical cancer cells by regulating miR-129 expression and to evaluate the potential value of miR-129 as a diagnostic and prognostic biomarker. This study found that the expression level of miR-129 in HPV-related cervical cancer tissues was significantly higher than that in normal cervical tissues and its high expression was significantly correlated with tumor size, FIGO advanced stage and lymph node metastasis. This is consistent with previous research on cervical cancer and leukemia (Li *et al*., 2022; Wang *et al*., 2025). Survival analysis further confirmed that cases with high miR-129 expression had significantly shorter overall survival than those with low expression. Multivariate Cox regression analysis showed that high expression of miR-129 was an independent prognostic risk factor for OS (HR = 2.512, 95% CI: 1.232 - 5.124, P = 0.011). These results suggest that miR-129 may serve as an adverse prognostic biomarker for HPV-related cervical cancer. Notably, ROC curve analysis showed that the AUC for miR-129 expression in differentiating cervical cancer cases from normal controls was 0.788 (95% CI: 0.693 - 0.884), indicating moderate diagnostic value.

Article in press

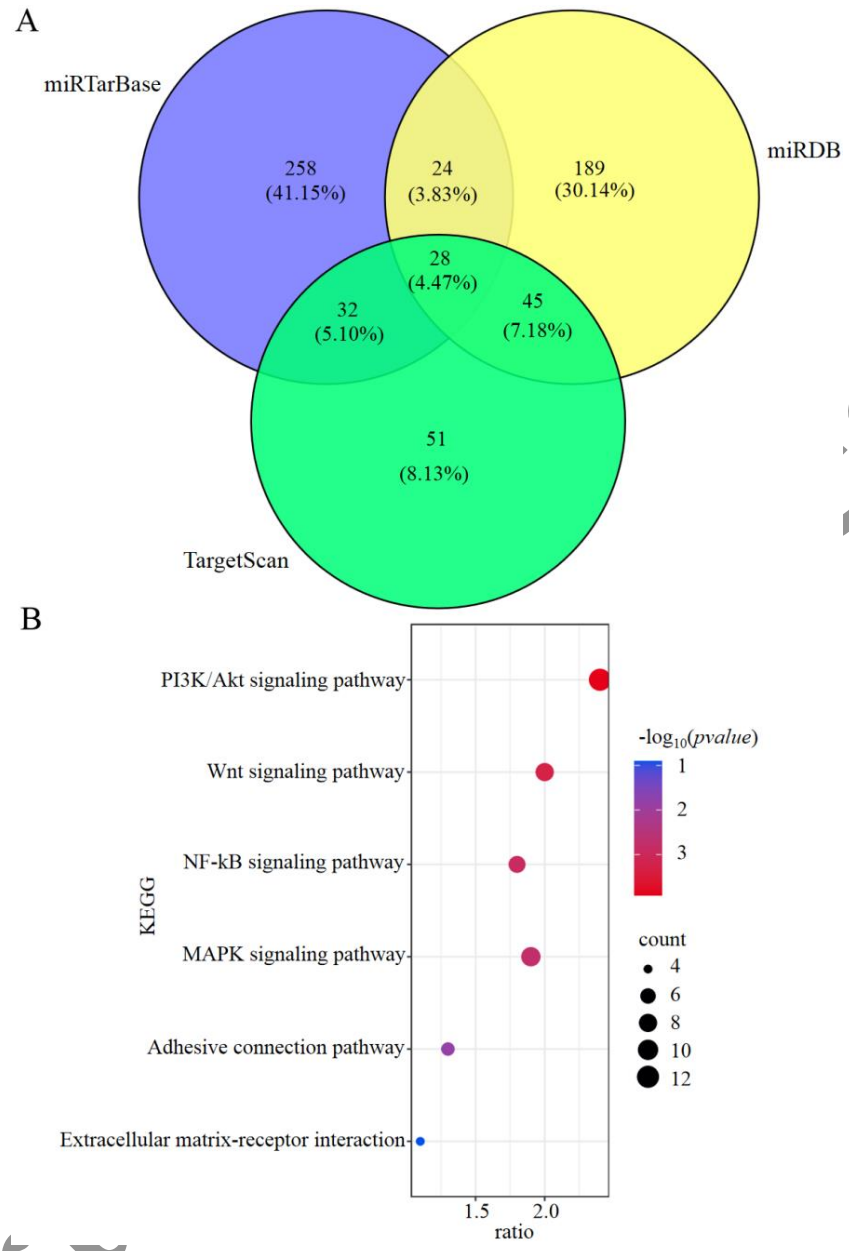


Fig. 6: Bioinformatics prediction of potential target genes and signaling pathways of miR-129.
A: Venn diagram showing the intersection of miR-129-5p target genes predicted by TargetScan, miRDB and miRTarBase databases (28 genes in common); B: KEGG pathway enrichment analysis bubble plot of the predicted target genes, including PI3K/Akt, Wnt, NF-κB, MAPK, adhesive connection and ECM-receptor interaction pathways ($P < 0.05$).

The optimal cutoff value determined by the Youden index was 1.85, at which the sensitivity was 76.9% and the specificity was 70.4%. The clinical significance of this cutoff value lies in: when the expression level of miR-129 in the patient's tissue is ≥1.85, the risk of developing cervical cancer significantly increases and the patient is more likely to present with aggressive clinical pathological features. However, the diagnostic efficacy of miR-129 alone is insufficient to replace existing screening methods. In the future, it may be considered to combine miR-129 with other molecular markers for detection to improve diagnostic accuracy.

This study found that co-culture with BMSCs significantly upregulated miR-129 expression in SiHa and HeLa cells. This result suggests that BMSCs may activate miR-129 transcription in cervical cancer cells by secreting soluble factors. Previous studies (Wang *et al*., 2023) have shown that exosomes derived from BMSCs can carry various miRNAs into tumor cells and regulate their gene expression. Additionally, cell factors, such as TGF-β and IL-6 secreted by BMSCs, may indirectly upregulate miR-129 expression by activating NF-κB or STAT3 signaling pathways (Tian *et al*., 2025; Pan *et al*., 2022). In this study, BMSCs and cervical cancer cells were co-cultured using a

Transwell non-contact system, thereby excluding direct cell contact and further supporting the regulatory mechanism mediated by soluble factors. However, the specific molecular mechanism by which BMSCs upregulate miR-129 still needs to be verified in subsequent experiments. In functional experiments, overexpression of miR-129 significantly enhanced the proliferation, colony formation and invasion ability of cervical cancer cells, while knockdown of miR-129 produced the opposite effect. These results are consistent with the pro-tumor role of miR-129 in cervical cancer (Huseinovic *et al*., 2024). Western blot results showed that after overexpression of miR-129, E-cadherin expression significantly decreased, while N-cadherin and MRP1 expression significantly increased, which was in line with the classic EMT phenotypic characteristics (Xu *et al*., 2024). EMT is a key step in tumor cells acquiring migration and invasion abilities, and it is also an important mechanism of chemotherapy resistance (Liaghat *et al*., 2024; Fedele *et al*., 2022). The regulatory effect of miR-129 on EMT in this study is highly consistent with its impact on cell invasion ability, further supporting the hypothesis that miR-129 promotes cervical cancer progression by inducing EMT. To verify whether the effect of BMSCs on cervical cancer cells depends on miR-129, this study conducted a miR-129 knockdown experiment simultaneously in the co-culture system. The results showed that knockdown of miR-129 could partially reverse the downregulation of E-cadherin and the upregulation of N-cadherin and MRP1 induced by BMSCs. This result indicates that the influence of BMSCs on EMT and MRP1 expression in cervical cancer cells is at least partially dependent on miR-129 upregulation. However, the expression levels of various proteins in the BMSCs + miR-129 inhibitor group did not fully return to the levels observed in the control group, suggesting that BMSCs may also exert their effects through other miRNAs or signaling pathways. Bioinformatics prediction revealed that the potential target genes of miR-129 were significantly enriched in signaling pathways, including PI3K/Akt, Wnt, NF-κB, and MAPK. These pathways play crucial roles in the occurrence, progression, EMT and drug resistance of cervical cancer. It is noteworthy that the adhesion junction pathway and ECM-receptor interaction pathway were also significantly enriched, which is highly consistent with the observed EMT phenotypic changes in this study.

However, the BMSCs used in this study were derived from SD rats. The cross-species co-culture model cannot fully simulate the human tumor microenvironment and the conclusion needs to be verified using human-derived BMSCs. At the same time, this study detected only MRP1 protein expression and did not conduct functional drug-resistance experiments, which cannot directly yield conclusions about the drug-resistance phenotype. Moreover, the Cox regression analysis did not adequately control confounding factors and the results may be biased. The bioinformatics prediction in this study was not verified by dual-luciferase reporter gene or pathway inhibitor experiments; it was based solely on an assumption. Its scientificity still needs further verification; and there is a lack of *in-vivo* animal experiments, so the translational significance is not yet clear.

This study has several limitations. First, the BMSCs used in this study were derived from SD rats. The cross-species co-culture model cannot fully simulate the human tumor microenvironment and the conclusion needs to be verified using human-derived BMSCs. Second, this study detected only MRP1 protein expression and did not conduct functional drug-resistance experiments, which cannot directly yield conclusions about the drug-resistance phenotype. Third, although the multivariate Cox regression analysis adjusted for major clinicopathological confounders, residual confounding from unmeasured factors (e.g., HPV viral load, immune status, or treatment variations) cannot be completely excluded. Regarding missing data, all 77 cervical cancer cases and 30 normal controls had complete clinicopathological and follow-up data, with no missing values for the variables included in the analysis. However, due to the retrospective design and reliance on the tissue bank, data on HPV viral load, detailed treatment regimens, and patient comorbidities were not uniformly available and were therefore not included in this analysis. Additionally, for a small subset of cases (n=7, 9.1%), detailed information on adjuvant therapy was incomplete; these cases were excluded from sensitivity analyses but included in the main analysis as their exclusion did not materially change the effect estimates (data not shown). Fourth, the bioinformatics prediction in this study was not verified by dual-luciferase reporter gene or pathway inhibitor experiments; it was based solely on an assumption. Its scientificity still needs further verification. Fifth, there is a lack of in-vivo animal experiments, so the translational significance is not yet clear. Additionally, the relatively small sample size of 77 cases from a single institution limits the generalizability of the findings, and the diagnostic performance of miR-129 (AUC=0.788) was evaluated without an external validation cohort, which may overestimate its clinical utility.

CONCLUSION

In conclusion, miR-129 is highly expressed in HPV-related cervical cancer and is significantly associated with poor patient prognosis. It has moderate diagnostic value for cervical cancer. BMSCs can induce EMT in cervical cancer cells and upregulate MRP1 expression by increasing miR-129 expression, thereby promoting tumor progression. This study provides a new perspective for understanding the molecular mechanism by which the tumor microenvironment regulates the progression of cervical cancer. The BMSCs/miR-129 axis may become a potential therapeutic target for cervical cancer.

Article in Press

Acknowledgments
We gratefully acknowledge Women's Hospital, School of Medicine, Zhejiang University for providing the necessary equipment and facilities for this study. We thank the Department of Pathology for their assistance with tissue sample collection and histological evaluation. We also thank the Laboratory Animal Center of Zhejiang University for providing technical support for animal experiments. We appreciate the valuable suggestions and critical comments from the reviewers and editors. All cases who participated in this study are sincerely acknowledged for their cooperation.

Author's contributions
Nieying Ma: Conceptualization, Methodology, Investigation, Data curation, Formal analysis, Writing – original draft, Visualization. The author designed the study and performed cell culture, transfection, co-culture experiments, qRT-PCR, Western blot, CCK-8, colony formation, and Transwell invasion assays. The author also collected clinical tissue samples, conducted statistical analyses (including ROC curves, survival analysis, and Cox regression), and prepared all Figs. and tables and wrote the initial draft of the manuscript; Kaijie Xu: Methodology, Validation, Investigation, Data curation, Writing – review and editing. The author assisted in validating experimental methods, independently verified data for cell proliferation, colony formation, and invasion assays, performed replicate qRT-PCR and Western blot experiments, provided literature support for the introduction and discussion sections, reviewed and revised the manuscript for methodological accuracy, and assisted in organizing the Figs. and tables; Zhize Wang: Conceptualization, Supervision, Project administration, Funding acquisition, Writing – review and editing, Validation. The author conceived the core scientific hypothesis (the BMSCs/miR-129 axis in HPV-associated cervical cancer), supervised the overall research design and project execution, secured funding and institutional ethical approval, interpreted the data and constructed the mechanistic model through bioinformatics analysis (target gene prediction and KEGG pathway enrichment), critically revised and finalized the manuscript for intellectual content, handled journal submission and correspondence with editors and reviewers and ensured compliance with ethical standards and data availability policies. All authors have read and approved the final version of the manuscript.

Funding
This study was conducted with institutional support from Women's Hospital, School of Medicine, Zhejiang University and The First Affiliated Hospital, Zhejiang University School of Medicine. No external funding from commercial or non-commercial funding bodies was received for this research. The authors' contributions to funding acquisition refer to the internal institutional resources and administrative support that made this study possible.

Data availability statement
The datasets generated during and/or analysed during the current study are available from the corresponding author on reasonable request.

Ethical approval
This study was approved by the Ethics Committee of Women's Hospital, School of Medicine, Zhejiang University (approval number: ZJU-2025-045). All procedures involving human participants were performed in accordance with the ethical standards of the institutional research committee and with the 1964 Helsinki Declaration and its later amendments. Informed consent was obtained from all individual participants included in the study. All animal experiments were conducted in accordance with the Guide for the Care and Use of Laboratory Animals published by the National Institutes of Health and were approved by the Animal Care and Use Committee of Zhejiang University (license number: 2025-889). All efforts were made to minimize animal suffering and reduce the number of animals used. This study was performed in adherence with the STROBE guidelines. See supplementary file for the STROBE checklist.

Conflict of interest
The authors declare that there are no conflicts of interest regarding the publication of this paper. No financial or personal relationships have influenced the design, execution, or reporting of this study. All authors have approved the final version of the manuscript and agree to its submission.

REFERENCES

Abas BI, Demirbolat GM and Cevik O (2022). Wharton jelly-derived mesenchymal stem cell exosomes induce apoptosis and suppress EMT signaling in cervical cancer cells as an effective drug carrier system of paclitaxel. *PLoS One*., **17**(9): e0274607.

Bergman H, Henschke N, Arevalo-Rodriguez I, Buckley BS, Crosbie EJ, Davies JC, Dwan K, Golder SP, Loke YK, Probyn K, Petkovic J, Villanueva G and Morrison J (2025). Human papillomavirus (HPV) vaccination for the prevention of cervical cancer and other HPV-related diseases: A network meta-analysis. *Cochrane Database Syst. Rev*., **11**(11): CD015364.

Bujang MA and Adnan TH (2016). Requirements for minimum sample size for sensitivity and specificity analysis. *J. Clin. Diagn. Res*., **10**(10): YE01-YE06.

Cortes-Morales VA, Chavez-Sanchez L, Rocha-Zavaleta L, Espindola-Garibay S, Monroy-Garcia A, Castro-Manrreza ME, Fajardo-Orduna GR, Apresa-García T, Gutiérrez-de la Barrera M, Mayani H and Montesinos JJ (2023). Mesenchymal stem/stromal cells derived from cervical cancer promote M2 macrophage polarization. *Cells*., **12**(7): 1047.

Gao Q, Wang L, Wang S, Huang B, Jing Y and Su J (2022). Bone marrow mesenchymal stromal cells: Identification,

In press

classification and differentiation. *Front. Cell Dev. Biol*., **9**: 787118.

Fedele M, Sgarra R, Battista S, Cerchia L and Manfioletti G (2022). The epithelial-mesenchymal transition at the crossroads between metabolism and tumor progression. *Int. J. Mol. Sci*., **23**(2): 800.

Hong X and He SL (2025). lncRNA LINC00958 activates NOTCH3 by competitively inhibiting miR-129-2-3p to exacerbate the malignant biological behaviors of endometrial cancer cells. *Kaohsiung J. Med. Sci*., **41**(12): e70081.

Hong Y, Xiang L, Hu Y, Zhou Z, Yu H and Zhu B (2012). Interstitial magnetic resonance lymphography is an effective diagnostic tool for the detection of lymph node metastases in patients with cervical cancer. *BMC Cancer*., **12**: 360.

Huseinovic A, Xu M, Jaspers A, Bais B and Steenbergen RDM (2024). miR-129-5p inhibits anchorage-independent growth through silencing of ACTN1 and the ELK4/c-FOS axis in HPV-transformed keratinocytes. *J Med Virol*., **96**(4): e29580.

Intan NS, Utama R, Wulandari D, Wisdharilla R, Khanza SM, Ramadhan MR, Widyahening IS, Nurainy N, Sari RM and Andrijono (2025). Urinary detection of high-risk HPV DNA to enhance cervical cancer screening in developing countries. *Microbiol Spectr*., **13**(9): e0193824.

Jeong J, Mun S, Oh Y, Cho CS, Yun K, Ahn Y, Chung WH, Lim MY, Lee KE, Hwang TS and Han K (2022). A qRT-PCR method capable of quantifying specific microorganisms compared to NGS-based metagenome profiling data. *Microorganisms*., **10**(2): 324.

Kusakabe M, Taguchi A, Sone K, Mori M and Osuga Y (2023). Carcinogenesis and management of human papillomavirus-associated cervical cancer. *Int J Clin Oncol*., **28**(8): 965-974.

Laughlin-Tommaso SK, Hesley GK, Hopkins MR, Brandt KR, Zhu Y and Stewart EA (2017). Clinical limitations of the international federation of gynecology and obstetrics (FIGO) classification of uterine fibroids. *Int J Gynaecol Obstet*., **139**(2): 143-148.

Leventakou D, Gouloumi AR, Spathis A, Pouliakis A, Koufopoulos N, Pergialiotis V, Drakakis P, Panayiotides IG and Kottaridi C (2023). Expression profile of miRNAs computationally predicted to target PDL-1 in cervical tissues of different histology groups. *Front Cell Dev Biol*., **11**: 1101041.

Li Y and Dou S (2022). FLOT2 Promotes the proliferation and epithelial-mesenchymal transition of cervical cancer by activating the MEK/ERK1/2 pathway. *Balkan Med J*., **39**(4): 267-274.

Li H, Bi K, Feng S, Wang Y and Zhu C (2022). CircRNA CircEHBP1 regulates the maturation of MiR-129 to increase the chemoresistance of cancer cells to adriamycin in acute myeloid leukaemia. *Mediterr J Hematol Infect Dis*., **14**(1): e2022062.

Liaghat M, Ferdousmakan S, Mortazavi SH, Yahyazadeh S, Irani A, Banihashemi S, Seyedi Asl FS, Akbari A, Farzam F, Aziziyan F, Bakhtiyari M, Arghavani MJ, Zalpoor H and Nabi-Afjadi M (2024). The impact of epithelial-mesenchymal transition (EMT) induced by metabolic processes and intracellular signaling pathways on chemo-resistance, metastasis and recurrence in solid tumors. *Cell Commun Signal*., **22**(1): 575.

Liao Y, Huang J, Liu P, Zhang C, Liu J, Xia M, Shang C, Ooi S, Chen Y, Qin S, Du Q, Liu T, Xu M, Zou Q, Zhou Y, Huang H, Pan Y, Wang W and Yao S (2022). Downregulation of LNMAS orchestrates partial EMT and immune escape from macrophage phagocytosis to promote lymph node metastasis of cervical cancer. *Oncogene*., **41**(13): 1931-1943.

Maiorano MFP, Cazzolla A, Maiorano BA, Loizzi V, Cormio G, Colonna G and Lopez S (2026). Impact of HPV vaccine on CIN2+ recurrence after conization: A systematic review and meta-analysis of vaccination timing, valency and surgical margins. *Front Oncol*., **16**: 1748972.

Mishra V (2022). Dot-blotting: A quick method for expression analysis of recombinant proteins. *Curr Protoc*., **2**(9): e546.

Mune G, Asefa A, Chillo SL and Woldesemayat EM (2026). Cervical cancer screening and associated factors among women of reproductive age in sidama regional state of ethiopia: A cross-sectional survey. *Cancer Rep*., **9**(2): e70498.

Nittayaboon K, Molika P, Bissanum R, Leetanaporn K, Chumsuwan N and Navakanitworakul R (2025). Bone marrow mesenchymal stem cell-derived exosomes modulate chemoradiotherapy response in cervical cancer spheroids. *Pharmaceuticals*., **18**(7): 1050.

Nygard M, Røysland K, Campbell S and Dillner J (2014). Comparative effectiveness study on human papillomavirus detection methods used in the cervical cancer screening programme. *BMJ Open*., **4**(1): e003460.

Pan Y, Wang T, Zhao Z, Wei W, Yang X, Wang X and Xin W (2022). Novel insights into the emerging role of neat 1 and its effects downstream in the regulation of inflammation. *J Inflamm Res*., **15**: 557-571.

Popiel-Kopaczyk A, Piotrowska A, Sputa-Grzegrzolka P, Smolarz B, Romanowicz H, Dziegiel P, Podhorska-Okolow M and Kobierzycki C (2023). The immunohistochemical expression of epithelial-mesenchymal transition markers in precancerous lesions and cervical cancer. *Int J Mol Sci*., **24**(9): 8063.

Sawaya GF and Smith-McCune K (2016). Cervical Cancer Screening. *Obstet Gynecol*., **127**(3): 459-467.

Tian H, Chen A, Gao P, Wang F, Zhao Y, Wang F, Lian C and Zhang Q (2025). Human umbilical cord mesenchymal stem cell-derived exosomes induce macrophage M2 polarization by antagonizing LPS-mediated stimulation of the NF-κB and STAT3 pathways. *Comb Chem High Throughput Screen*.,

Article in Press

28(10): 1766-1775.

Tu A, Wu H, Wang J, Hou X, Wang M, Jiang M and Zhou X (2025). Hypermethylation of miR-129-2-3p inhibits esophageal cancer proliferation and migration by down-regulating PPP6C expression. *Am J Transl Res*., **17**(2): 1459-1469.

Wang H, Sidike D, Liu P, Suo L and Niyazi H (2025). miR-129-5p regulates HMGB1/RAGE axis to inhibit pyroptosis and ameliorate cervical epithelial cell deterioration. *Eur J Histochem*., **69**(4): 4238.

Wang KH, Chang YH and Ding DC (2024). Bone marrow mesenchymal stem cells promote ovarian cancer cell proliferation via cytokine interactions. *Int J Mol Sci*., **25**(12): 6746.

Wang H, Zhou Z, Lin W, Qian Y, He S and Wang J (2023). MicroRNA-21 promotes head and neck squamous cell carcinoma (HNSCC) induced transition of bone marrow mesenchymal stem cells to cancer-associated fibroblasts. *BMC Cancer*., **23**(1): 1135.

Xu Z, Zhang Y, Dai H and Han B (2022). Epithelial-mesenchymal transition-mediated tumor therapeutic resistance. *Molecules*., **27**(15): 4750.

Xu Y, Tang Y, Xu Q and He W (2024). TMEM97 knockdown inhibits 5-fluorouracil resistance by regulating epithelial-mesenchymal transition and ABC transporter expression via inactivating the Akt/mTOR pathway in 5-fluorouracil-resistant colorectal cancer cells. *Chem Biol Drug Des*., **103**(2): e14490.

Zhang M, Hong X, Ma N, Wei Z, Ci X and Zhang S (2023). The promoting effect and mechanism of Nrf2 on cell metastasis in cervical cancer. *J Transl Med*., **21**(1): 433.

Article in Press